

## Chapter 9

# Dirichlet–Voronoi Diagrams and Delaunay Triangulations

### 9.1 Dirichlet–Voronoi Diagrams

In this chapter we present very briefly the concepts of a Voronoi diagram and of a Delaunay triangulation.

These are important tools in computational geometry, and Delaunay triangulations are important in problems where it is necessary to fit 3D data using surface splines.

It is usually useful to compute a good mesh for the projection of this set of data points onto the  $xy$ -plane, and a Delaunay triangulation is a good candidate.

Our presentation will be rather sketchy. We are primarily interested in defining these concepts and stating their most important properties without proofs.

For a comprehensive exposition of Voronoi diagrams, Delaunay triangulations, and more topics in computational geometry, consult O’Rourke [?], Preparata and Shamos [?], Boissonnat and Yvinec [?], de Berg, Van Kreveld, Overmars, and Schwarzkopf [?], or Risler [?].

The survey by Graham and Yao [?] contains a very gentle and lucid introduction to computational geometry.

For concreteness, one may safely assume that we work in the affine space  $\mathcal{E} = \mathbb{E}^m$ , although what follows applies to any Euclidean space of finite dimension.

Given a set  $P = \{p_1, \dots, p_n\}$  of  $n$  points in  $\mathcal{E}$ , it is often useful to find a partition of the space  $\mathcal{E}$  into regions each containing a single point of  $P$  and having some nice properties.

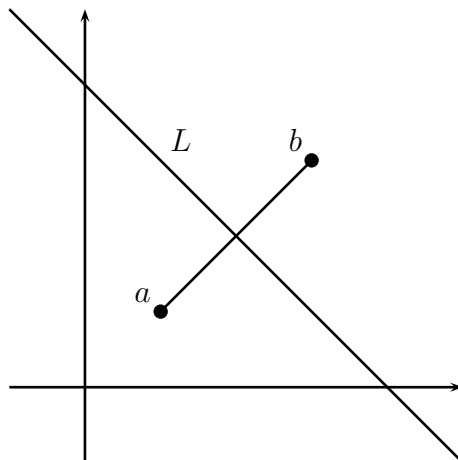
It is also often useful to find triangulations of the convex hull of  $P$  having some nice properties.

We shall see that this can be done and that the two problems are closely related. In order to solve the first problem, we need to introduce bisector lines and bisector planes.

For simplicity, let us first assume that  $\mathcal{E}$  is a plane i.e., has dimension 2.

Given any two distinct points  $a, b \in \mathcal{E}$ , the line orthogonal to the line segment  $(a, b)$  and passing through the midpoint of this segment is the locus of all points having equal distance to  $a$  and  $b$ .

It is called the *bisector line of  $a$  and  $b$* . The bisector line of two points is illustrated in Figure 9.1.

Figure 9.1: The bisector line  $L$  of  $a$  and  $b$ 

If  $h = \frac{1}{2}a + \frac{1}{2}b$  is the midpoint of the line segment  $(a, b)$ , letting  $m$  be an arbitrary point on the bisector line, the equation of this line can be found by writing that  $\mathbf{hm}$  is orthogonal to  $\mathbf{ab}$ .

In any orthogonal frame, letting  $m = (x, y)$ ,  $a = (a_1, a_2)$ ,  $b = (b_1, b_2)$ , the equation of this line can be written as

$$(b_1 - a_1)x + (b_2 - a_2)y = (b_1^2 + b_2^2)/2 - (a_1^2 + a_2^2)/2.$$

The closed half-plane  $H(a, b)$  containing  $a$  and with boundary the bisector line is the locus of all points such that

$$(b_1 - a_1)x + (b_2 - a_2)y \leq (b_1^2 + b_2^2)/2 - (a_1^2 + a_2^2)/2,$$

and the closed half-plane  $H(b, a)$  containing  $b$  and with boundary the bisector line is the locus of all points such that

$$(b_1 - a_1)x + (b_2 - a_2)y \geq (b_1^2 + b_2^2)/2 - (a_1^2 + a_2^2)/2.$$

The closed half-plane  $H(a, b)$  is the set of all points whose distance to  $a$  is less than or equal to the distance to  $b$ , and vice versa for  $H(b, a)$ . Thus, points in the closed half-plane  $H(a, b)$  are closer to  $a$  than they are to  $b$ .

We now consider a problem called the *post office problem* by Graham and Yao [?].

Given any set  $P = \{p_1, \dots, p_n\}$  of  $n$  points in the plane (considered as *post offices* or *sites*), for any arbitrary point  $x$ , find out which post office is closest to  $x$ .

Since  $x$  can be arbitrary, it seems desirable to precompute the sets  $V(p_i)$  consisting of all points that are closer to  $p_i$  than to any other point  $p_j \neq p_i$ .

Indeed, if the sets  $V(p_i)$  are known, the answer is any post office  $p_i$  such that  $x \in V(p_i)$ .

Thus, it remains to compute the sets  $V(p_i)$ . For this, if  $x$  is closer to  $p_i$  than to any other point  $p_j \neq p_i$ , then  $x$  is on the same side as  $p_i$  with respect to the bisector line of  $p_i$  and  $p_j$  for every  $j \neq i$ , and thus

$$V(p_i) = \bigcap_{j \neq i} H(p_i, p_j).$$

If  $\mathcal{E}$  has dimension 3, the locus of all points having equal distance to  $a$  and  $b$  is a plane. It is called the *bisector plane of  $a$  and  $b$* .

The equation of this plane is also found by writing that  $\mathbf{hm}$  is orthogonal to  $\mathbf{ab}$ . The equation of this plane can be written as

$$(b_1 - a_1)x + (b_2 - a_2)y + (b_3 - a_3)z = \\ (b_1^2 + b_2^2 + b_3^2)/2 - (a_1^2 + a_2^2 + a_3^2)/2.$$

The closed half-space  $H(a, b)$  containing  $a$  and with boundary the bisector plane is the locus of all points such that

$$(b_1 - a_1)x + (b_2 - a_2)y + (b_3 - a_3)z \leq \\ (b_1^2 + b_2^2 + b_3^2)/2 - (a_1^2 + a_2^2 + a_3^2)/2,$$

and the closed half-space  $H(b, a)$  containing  $b$  and with boundary the bisector plane is the locus of all points such that

$$(b_1 - a_1)x + (b_2 - a_2)y + (b_3 - a_3)z \geq \\ (b_1^2 + b_2^2 + b_3^2)/2 - (a_1^2 + a_2^2 + a_3^2)/2.$$

The closed half-space  $H(a, b)$  is the set of all points whose distance to  $a$  is less than or equal to the distance to  $b$ , and vice versa for  $H(b, a)$ . Again, points in the closed half-space  $H(a, b)$  are closer to  $a$  than they are to  $b$ .

Given any set  $P = \{p_1, \dots, p_n\}$  of  $n$  points in  $\mathcal{E}$  (of dimension  $m = 2, 3$ ), it is often useful to find for every point  $p_i$  the region consisting of all points that are closer to  $p_i$  than to any other point  $p_j \neq p_i$ , that is, the set

$$V(p_i) = \{x \in \mathcal{E} \mid d(x, p_i) \leq d(x, p_j), \text{ for all } j \neq i\},$$

where  $d(x, y) = (\mathbf{x}y \cdot \mathbf{x}y)^{1/2}$ , the Euclidean distance associated with the inner product  $\cdot$  on  $\mathcal{E}$ .

From the definition of the bisector line (or plane), it is immediate that

$$V(p_i) = \bigcap_{j \neq i} H(p_i, p_j).$$

Families of sets of the form  $V(p_i)$  were investigated by Dirichlet [?] (1850) and Voronoi [?] (1908). Voronoi diagrams also arise in crystallography (Gilbert [?]).

Other applications, including facility location and path planning, are discussed in O'Rourke [?]. For simplicity, we also denote the set  $V(p_i)$  by  $V_i$ , and we introduce the following definition.

**Definition 9.1.1** Let  $\mathcal{E}$  be a Euclidean space of dimension  $m \geq 1$ . Given any set  $P = \{p_1, \dots, p_n\}$  of  $n$  points in  $\mathcal{E}$ , the *Dirichlet–Voronoi diagram*  $\mathcal{V}(P)$  of  $P = \{p_1, \dots, p_n\}$  is the family of subsets of  $\mathcal{E}$  consisting of the sets  $V_i = \bigcap_{j \neq i} H(p_i, p_j)$  and of all of their intersections.

Dirichlet–Voronoi diagrams are also called *Voronoi diagrams*, *Voronoi tessellations*, or *Thiessen polygons*. Following common usage, we will use the terminology *Voronoi diagram*.

As intersections of convex sets (closed half-planes or closed half-spaces), the *Voronoi regions*  $V(p_i)$  are convex sets. In dimension two, the boundaries of these regions are convex polygons, and in dimension three, the boundaries are convex polyhedra.

Whether a region  $V(p_i)$  is bounded or not depends on the location of  $p_i$ .

If  $p_i$  belongs to the boundary of the convex hull of the set  $P$ , then  $V(p_i)$  is unbounded, and otherwise bounded.

In dimension two, the convex hull is a convex polygon, and in dimension three, the convex hull is a convex polyhedron.

As we will see later, there is an intimate relationship between convex hulls and Voronoi diagrams.

Generally, if  $\mathcal{E}$  is a Euclidean space of dimension  $m$ , given any two distinct points  $a, b \in \mathcal{E}$ , the locus of all points having equal distance to  $a$  and  $b$  is a hyperplane.

It is called the *bisector hyperplane of  $a$  and  $b$* . The equation of this hyperplane is still found by writing that  $\mathbf{hm}$  is orthogonal to  $\mathbf{ab}$ . The equation of this hyperplane can be written as

$$(b_1 - a_1)x_1 + \cdots + (b_m - a_m)x_m = \\ (b_1^2 + \cdots + b_m^2)/2 - (a_1^2 + \cdots + a_m^2)/2.$$

The closed half-space  $H(a, b)$  containing  $a$  and with boundary the bisector hyperplane is the locus of all points such that

$$(b_1 - a_1)x_1 + \cdots + (b_m - a_m)x_m \leq \\ (b_1^2 + \cdots + b_m^2)/2 - (a_1^2 + \cdots + a_m^2)/2,$$

and the closed half-space  $H(b, a)$  containing  $b$  and with boundary the bisector hyperplane is the locus of all points such that

$$(b_1 - a_1)x_1 + \cdots + (b_m - a_m)x_m \geq \\ (b_1^2 + \cdots + b_m^2)/2 - (a_1^2 + \cdots + a_m^2)/2.$$

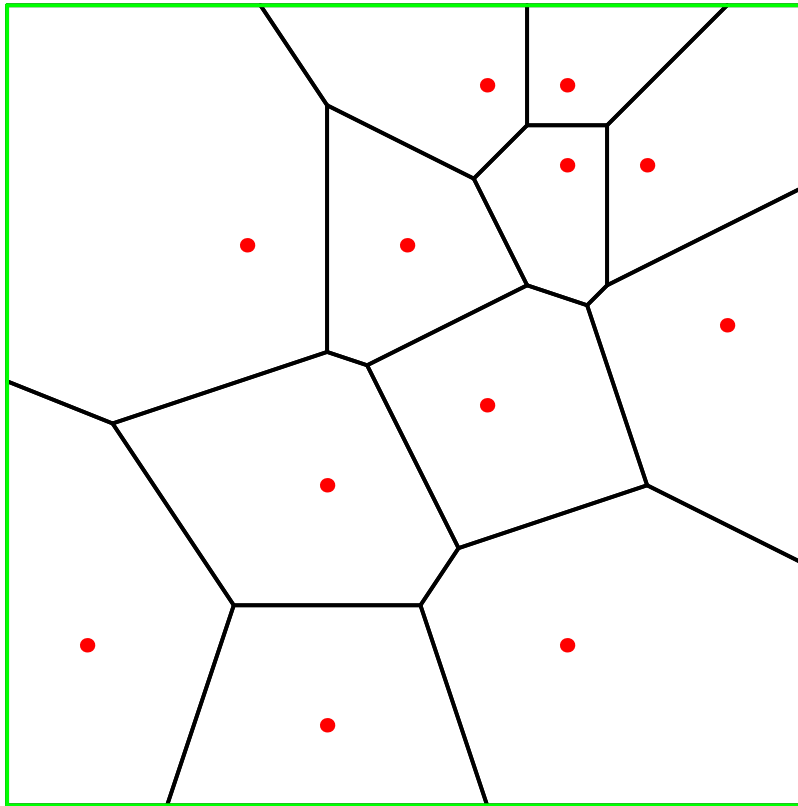


Figure 9.2: A Voronoi diagram

The closed half-space  $H(a, b)$  is the set of all points whose distance to  $a$  is less than or equal to the distance to  $b$ , and vice versa for  $H(b, a)$ .

Figure 9.2 shows the Voronoi diagram of a set of twelve points.

In the general case where  $\mathcal{E}$  has dimension  $m$ , the definition of the Voronoi diagram  $\mathcal{V}(P)$  of  $P$  is the same as Definition 9.1.1, except that  $H(p_i, p_j)$  is the closed half-space containing  $p_i$  and having the bisector hyperplane of  $a$  and  $b$  as boundary.

Also, observe that the convex hull of  $P$  is a convex polytope.

We will now state a lemma listing the main properties of Voronoi diagrams.

It turns out that certain degenerate situations can be avoided if we assume that if  $P$  is a set of points in an affine space of dimension  $m$ , then no  $m + 2$  points from  $P$  belong to the same  $(m - 1)$ -sphere.

We will say that the points of  $P$  are in *general position*.

Thus when  $m = 2$ , no 4 points in  $P$  are cocyclic, and when  $m = 3$ , no 5 points in  $P$  are on the same sphere.

**Lemma 9.1.2** *Given a set  $P = \{p_1, \dots, p_n\}$  of  $n$  points in some Euclidean space  $\mathcal{E}$  of dimension  $m$  (say  $\mathbb{E}^m$ ), if the points in  $P$  are in general position and not in a common hyperplane then the Voronoi diagram of  $P$  satisfies the following conditions:*

- (1) *Each region  $V_i$  is convex and contains  $p_i$  in its interior.*
- (2) *Each vertex of  $V_i$  belongs to  $m + 1$  regions  $V_j$  and to  $m + 1$  edges.*
- (3) *The region  $V_i$  is unbounded iff  $p_i$  belongs to the boundary of the convex hull of  $P$ .*
- (4) *If  $p$  is a vertex that belongs to the regions  $V_1, \dots, V_{m+1}$ , then  $p$  is the center of the  $(m - 1)$ -sphere  $S(p)$  determined by  $p_1, \dots, p_{m+1}$ . Furthermore, no point in  $P$  is inside the sphere  $S(p)$  (i.e., in the open ball associated with the sphere  $S(p)$ ).*
- (5) *If  $p_j$  is a nearest neighbor of  $p_i$ , then one of the faces of  $V_i$  is contained in the bisector hyperplane of  $(p_i, p_j)$ .*

(6)

$$\bigcup_{i=1}^n V_i = \mathcal{E}, \quad \text{and} \quad \overset{\circ}{V}_i \cap \overset{\circ}{V}_j = \emptyset, \quad \text{for all } i, j, i \neq j,$$

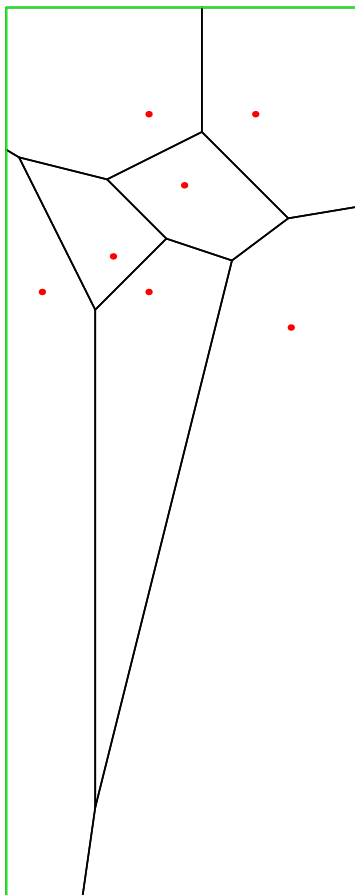


Figure 9.3: Another Voronoi diagram

where  $\overset{\circ}{V}_i$  denotes the interior of  $V_i$ .

For simplicity, let us again consider the case where  $\mathcal{E}$  is a plane. It should be noted that certain Voronoi regions, although closed, may extend very far.

Figure 9.3 shows such an example.

It is also possible for certain unbounded regions to have parallel edges.

There are a number of methods for computing Voronoi diagrams. A fairly simple (although not very efficient) method is to compute each Voronoi region  $V(p_i)$  by intersecting the half-planes  $H(p_i, p_j)$ .

One way to do this is to construct successive convex polygons that converge to the boundary of the region.

At every step we intersect the current convex polygon with the bisector line of  $p_i$  and  $p_j$ . There are at most two intersection points. We also need a starting polygon, and for this we can pick a square containing all the points.

A naive implementation will run in  $O(n^3)$ .

However, the intersection of half-planes can be done in  $O(n \log n)$ , using the fact that the vertices of a convex polygon can be sorted.

Thus, the above method runs in  $O(n^2 \log n)$ . Actually, there are faster methods (see Preparata and Shamos [?] or O'Rourke [?]), and it is possible to design algorithms running in  $O(n \log n)$ .

The most direct method to obtain fast algorithms is to use the “lifting method” discussed in Section 9.4, whereby the original set of points is lifted onto a paraboloid, and to use fast algorithms for finding a convex hull.

A very interesting (undirected) graph can be obtained from the Voronoi diagram as follows: The vertices of this graph are the points  $p_i$  (each corresponding to a unique region of  $\mathcal{V}(P)$ ), and there is an edge between  $p_i$  and  $p_j$  iff the regions  $V_i$  and  $V_j$  share an edge.

The resulting graph is called a *Delaunay triangulation* of the convex hull of  $P$ , after Delaunay, who invented this concept in 1934. Such triangulations have remarkable properties.

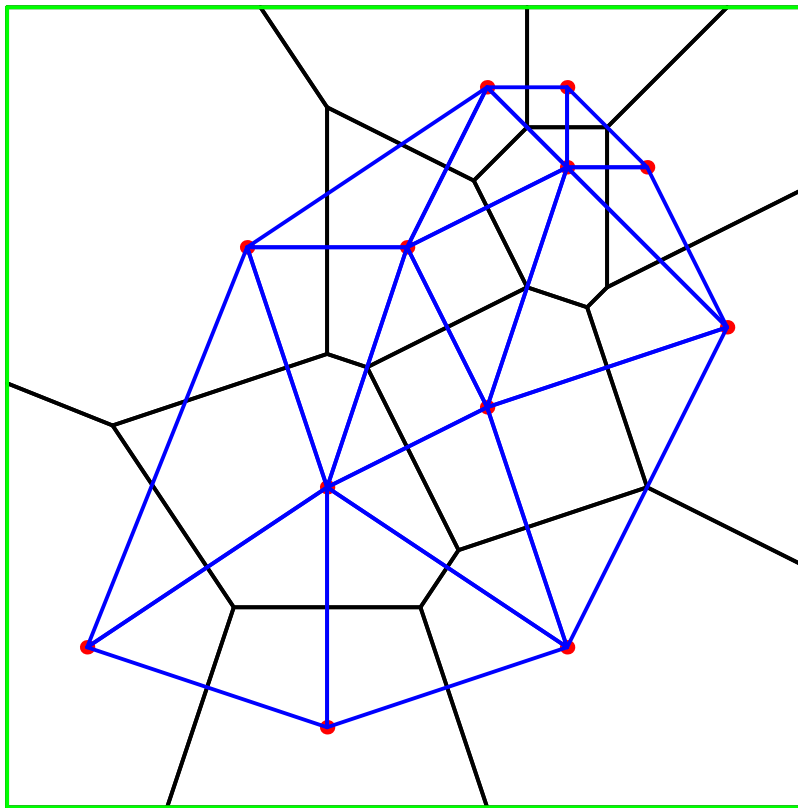


Figure 9.4: Delaunay triangulation associated with a Voronoi diagram

Figure 9.4 shows the Delaunay triangulation associated with the earlier Voronoi diagram of a set of twelve points.

One has to be careful to make sure that all the Voronoi vertices have been computed before computing a Delaunay triangulation, since otherwise, some edges could be missed.

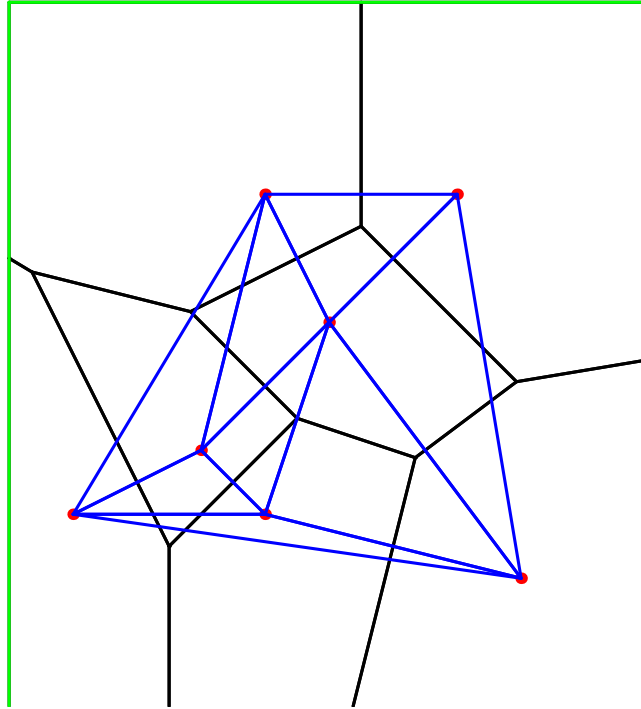


Figure 9.5: Another Delaunay triangulation associated with a Voronoi diagram

In Figure 9.5 illustrating such a situation, if the lowest Voronoi vertex had not been computed (not shown on the diagram!), the lowest edge of the Delaunay triangulation would be missing.

The concept of a triangulation can be generalized to dimension 3, or even to any dimension  $m$ .

## 9.2 Simplicial Complexes and Triangulations

The concept of a triangulation relies on the notion of pure simplicial complex defined in Chapter 7. For the reader's convenience, we repeat the relevant definitions.

**Definition 9.2.1** Let  $\mathcal{E}$  be any normed affine space, say  $\mathcal{E} = \mathbb{E}^m$  with its usual Euclidean norm. Given any  $n + 1$  affinely independent points  $a_0, \dots, a_n$  in  $\mathcal{E}$ , the  $n$ -simplex (or simplex)  $\sigma$  defined by  $a_0, \dots, a_n$  is the convex hull of the points  $a_0, \dots, a_n$ , that is, the set of all convex combinations  $\lambda_0 a_0 + \dots + \lambda_n a_n$ , where  $\lambda_0 + \dots + \lambda_n = 1$  and  $\lambda_i \geq 0$  for all  $i$ ,  $0 \leq i \leq n$ .

We call  $n$  the *dimension* of the  $n$ -simplex  $\sigma$ , and the points  $a_0, \dots, a_n$  are the *vertices* of  $\sigma$ .

Given any subset  $\{a_{i_0}, \dots, a_{i_k}\}$  of  $\{a_0, \dots, a_n\}$  (where  $0 \leq k \leq n$ ), the  $k$ -simplex generated by  $a_{i_0}, \dots, a_{i_k}$  is called a  $k$ -*face* or simply a *face* of  $\sigma$ .

A face  $s$  of  $\sigma$  is a *proper face* if  $s \neq \sigma$  (we agree that the empty set is a face of any simplex). For any vertex  $a_i$ , the face generated by  $a_0, \dots, a_{i-1}, a_{i+1}, \dots, a_n$  (i.e., omitting  $a_i$ ) is called the *face opposite*  $a_i$ .

Every face that is an  $(n - 1)$ -simplex is called a *boundary face* or *facet*. The union of the boundary faces is the *boundary of*  $\sigma$ , denoted by  $\partial\sigma$ .

It should be noted that for a 0-simplex consisting of a single point  $\{a_0\}$ ,  $\partial\{a_0\} = \emptyset$ .

Of course, a 0-simplex is a single point, a 1-simplex is the line segment  $(a_0, a_1)$ , a 2-simplex is a triangle  $(a_0, a_1, a_2)$  (with its interior), and a 3-simplex is a tetrahedron  $(a_0, a_1, a_2, a_3)$  (with its interior).

We now put simplices together to form more complex shapes. The intuition behind the next definition is that the building blocks should be “glued cleanly.”

**Definition 9.2.2** A *simplicial complex in  $\mathbb{E}^m$*  (for short, a *complex in  $\mathbb{E}^m$* ) is a set  $K$  consisting of a (finite or infinite) set of simplices in  $\mathbb{E}^m$  satisfying the following conditions:

- (1) Every face of a simplex in  $K$  also belongs to  $K$ .
- (2) For any two simplices  $\sigma_1$  and  $\sigma_2$  in  $K$ , if  $\sigma_1 \cap \sigma_2 \neq \emptyset$ , then  $\sigma_1 \cap \sigma_2$  is a common face of both  $\sigma_1$  and  $\sigma_2$ .

Every  $k$ -simplex,  $\sigma \in K$ , is called a *k-face* (or *face*) of  $K$ . A 0-face  $\{v\}$  is called a *vertex* and a 1-face is called an *edge*. The *dimension* of the simplicial complex  $K$  is the maximum of the dimensions of all simplices in  $K$ .

If  $\dim K = d$ , then every face of dimension  $d$  is called a *cell* and every face of dimension  $d - 1$  is called a *facet*.

Condition (2) guarantees that the various simplices forming a complex intersect nicely.

**Remarks:**

1. A simplicial complex,  $K$ , is a combinatorial object, namely, a *set* of simplices satisfying certain conditions but not a subset of  $\mathbb{E}^m$ . However, every complex,  $K$ , yields a subset of  $\mathbb{E}^m$  called the geometric realization of  $K$  and denoted  $|K|$ . This object will be defined shortly and should not be confused with the complex.

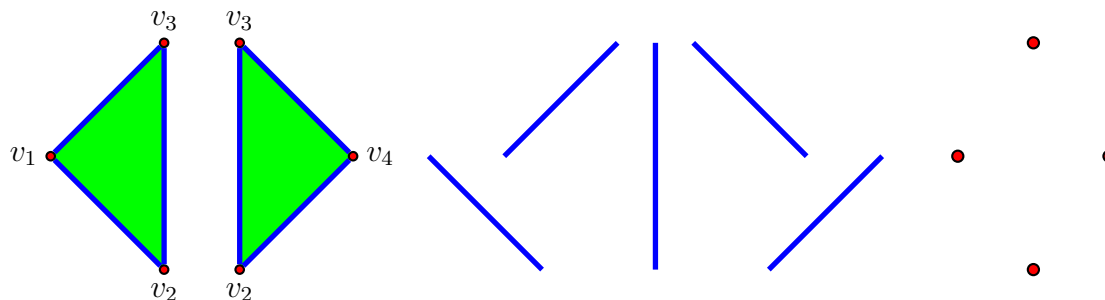


Figure 9.6: A set of simplices forming a complex

Figure 9.6 illustrates this aspect of the definition of a complex. For clarity, the two triangles (2-simplices) are drawn as disjoint objects even though they share the common edge,  $(v_2, v_3)$  (a 1-simplex) and similarly for the edges that meet at some common vertex.

2. It is important to note that in order for a complex,  $K$ , of dimension  $d$  to be realized in  $\mathbb{E}^m$ , the dimension of the “ambient space”  $m$ , must be big enough. For example, there are 2-complexes that can’t be realized in  $\mathbb{E}^3$  or even in  $\mathbb{E}^4$ . There has to be enough room in order for condition (2) to be satisfied. It is not hard to prove that  $m = 2d + 1$  is always sufficient. Sometimes,  $2d$  works, for example in the case of surfaces (where  $d = 2$ ).

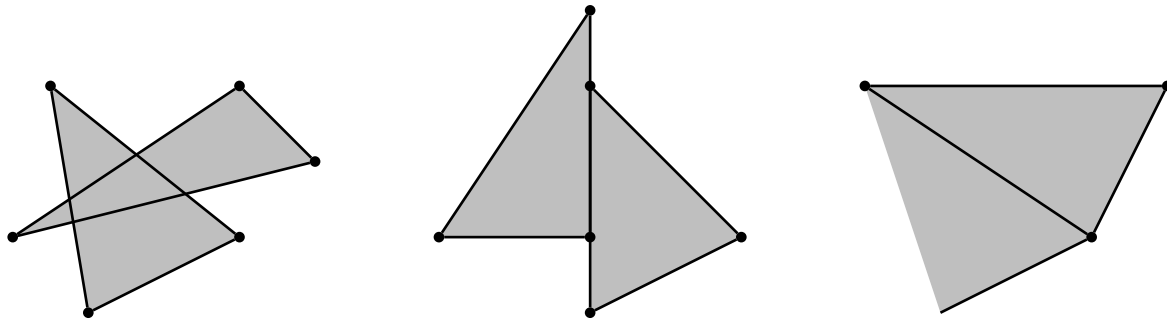


Figure 9.7: Collections of simplices not forming a complex

Some collections of simplices violating some of the conditions of Definition 9.2.2 are shown in Figure 9.7.

On the left, the intersection of the two 2-simplices is neither an edge nor a vertex of either triangle.

In the middle case, two simplices meet along an edge which is not an edge of either triangle.

On the right, there is a missing edge and a missing vertex.

The union  $|K|$  of all the simplices in  $K$  is a subset of  $\mathbb{E}^m$ .

The resulting space  $|K|$  is called the *geometric realization of  $K$* .

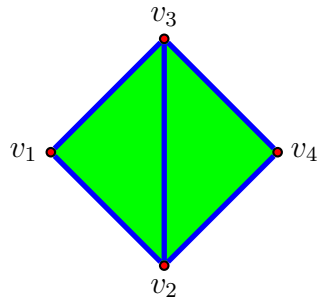


Figure 9.8: The geometric realization of the complex of Figure 9.6

The geometric realization of the complex from Figure 9.6 is shown in Figure 9.8.

Some “legal” simplicial complexes are shown in Figure 9.9.

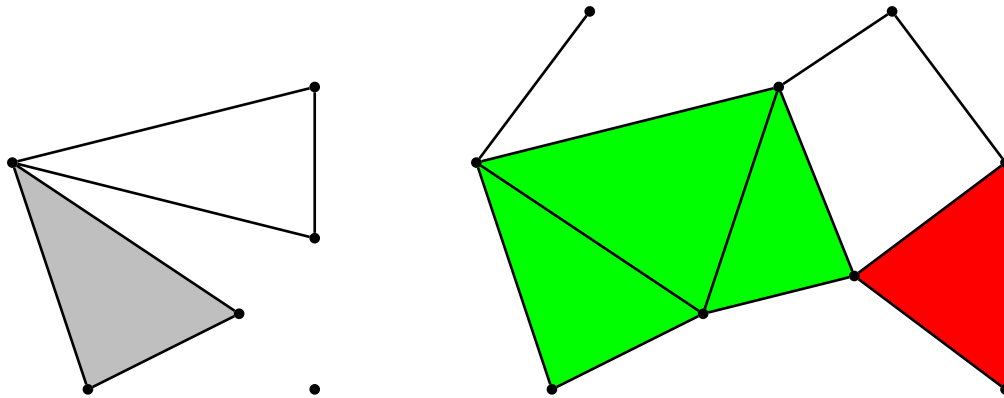


Figure 9.9: Examples of simplicial complexes

Obviously,  $|\sigma| = \sigma$  for every simplex,  $\sigma$ . Also, note that distinct complexes may have the same geometric realization. In fact, all the complexes obtained by subdividing the simplices of a given complex yield the same geometric realization.

A *polytope* is the geometric realization of some simplicial complex. A polytope of dimension 1 is usually called a *polygon*, and a polytope of dimension 2 is usually called a *polyhedron*.

In the sequel, we will consider only finite simplicial complexes, that is, complexes  $K$  consisting of a finite number of simplices.

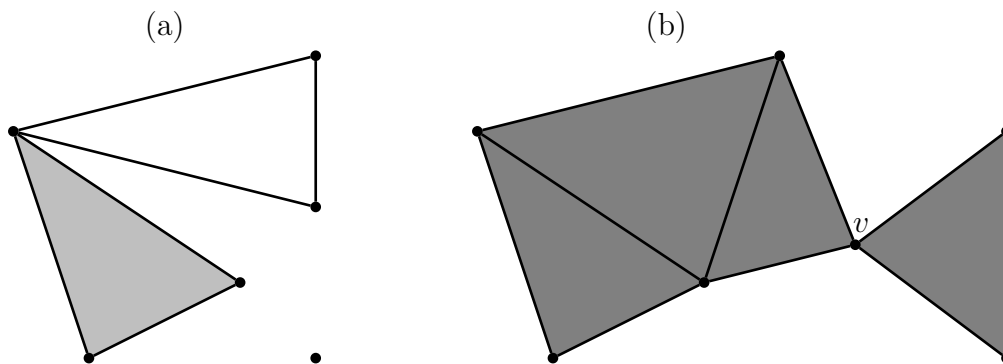


Figure 9.10: (a) A complex that is not pure. (b) A pure complex

A complex  $K$  of dimension  $d$  is *pure* (or *homogeneous*) iff every face of  $K$  is a face of some  $d$ -simplex of  $K$  (i.e., some cell of  $K$ ). A complex is *connected* iff  $|K|$  is connected.

The intuition behind the notion of a pure complex  $K$  of dimension  $d$  is that a pure complex is the result of gluing pieces all having the same dimension, namely  $d$ -simplices.

For example, in Figure 9.10, the complex on the left is not pure but the complex on the right is pure of dimension 2.

Most of the shapes that we will be interested in are well approximated by pure complexes, in particular, surfaces or solids.

We can now give a rigorous definition of a triangulation.

**Definition 9.2.3** Given a subset,  $S \subseteq \mathbb{E}^m$  (where  $m \geq 1$ ), a *triangulation of  $S$*  is a pure (finite) simplicial complex,  $K$ , of dimension  $m$  such that  $S = |K|$ , that is,  $S$  is equal to the geometric realization of  $K$ .

Given a finite set  $P$  of  $n$  points in the plane, and given a triangulation of the convex hull of  $P$  having  $P$  as its set of vertices, observe that the boundary of  $P$  is a convex polygon.

Similarly, given a finite set  $P$  of points in 3-space, and given a triangulation of the convex hull of  $P$  having  $P$  as its set of vertices, observe that the boundary of  $P$  is a convex polyhedron.

It is interesting to know how many triangulations exist for a set of  $n$  points (in the plane or in 3-space), and it is also interesting to know the number of edges and faces in terms of the number of vertices in  $P$ .

These questions can be settled using the Euler–Poincaré characteristic.

We say that a polygon in the plane is a *simple polygon* iff it is a connected closed polygon such that no two edges intersect (except at a common vertex).

**Lemma 9.2.4**

(1) *For any triangulation of a region of the plane whose boundary is a simple polygon, letting  $v$  be the number of vertices,  $e$  the number of edges, and  $f$  the number of triangles, we have the “Euler formula”*

$$v - e + f = 1.$$

(2) *For any region  $S$  in  $\mathbb{E}^3$  homeomorphic to a closed ball and for any triangulation of  $S$ , letting  $v$  be the number of vertices,  $e$  the number of edges,  $f$  the number of triangles, and  $t$  the number of tetrahedra, we have the “Euler formula”*

$$v - e + f - t = 1.$$

(3) *Furthermore, for any triangulation of the combinatorial surface,  $B(S)$ , that is the boundary of  $S$ , letting  $v'$  be the number of vertices,  $e'$  the number of edges, and  $f'$  the number of triangles, we have the “Euler formula”*

$$v' - e' + f' = 2.$$

*Proof.* All the statements are immediate consequences of Theorem 8.2.2.

For example, part (1) is obtained by mapping the triangulation onto a sphere using inverse stereographic projection, say from the North pole.

Then, we get a polytope on the sphere with an extra facet corresponding to the “outside” of the triangulation.

We have to deduct this facet from the Euler characteristic of the polytope and this is why we get 1 instead of 2.  $\square$

It is now easy to see that in case (1), the number of edges and faces is a linear function of the number of vertices and boundary edges, and that in case (3), the number of edges and faces is a linear function of the number of vertices.

If there are  $e_b$  edges in the boundary and  $e_i$  edges not in the boundary, we have

$$3f = e_b + 2e_i,$$

and together with

$$v - e_b - e_i + f = 1,$$

we get

$$\begin{aligned} v - e_b - e_i + e_b/3 + 2e_i/3 &= 1, \\ 2e_b/3 + e_i/3 &= v - 1, \end{aligned}$$

and thus,  $e_i = 3v - 3 - 2e_b$ . Since  $f = e_b/3 + 2e_i/3$ , we have  $f = 2v - 2 - e_b$ .

Similarly, since  $v' - e' + f' = 2$  and  $3f' = 2e'$ , we easily get  $e = 3v - 6$  and  $f = 2v - 4$ .

Thus, given a set  $P$  of  $n$  points, the number of triangles (and edges) for any triangulation of the convex hull of  $P$  using the  $n$  points in  $P$  for its vertices is fixed.

Case (2) is trickier, but it can be shown that

$$v - 3 \leq t \leq (v - 1)(v - 2)/2.$$

Thus, there can be different numbers of tetrahedra for different triangulations of the convex hull of  $P$ .

**Remark:** The numbers of the form  $v - e + f$  and  $v - e + f - t$  are called *Euler–Poincaré characteristics*.

They are topological invariants, in the sense that they are the same for all triangulations of a given polytope. This is a fundamental fact of algebraic topology.

We shall now investigate triangulations induced by Voronoi diagrams.

### 9.3 Delaunay Triangulations

Given a set  $P = \{p_1, \dots, p_n\}$  of  $n$  points in the plane and the Voronoi diagram  $\mathcal{V}(P)$  for  $P$ , we explained in Section 9.1 how to define an (undirected) graph:

The vertices of this graph are the points  $p_i$  (each corresponding to a unique region of  $\mathcal{V}(P)$ ), and there is an edge between  $p_i$  and  $p_j$  iff the regions  $V_i$  and  $V_j$  share an edge.

The resulting graph turns out to be a triangulation of the convex hull of  $P$  having  $P$  as its set of vertices. Such a complex can be defined in general.

For any set  $P = \{p_1, \dots, p_n\}$  of  $n$  points in  $\mathbb{E}^m$ , we say that a triangulation of the convex hull of  $P$  is *associated with*  $P$  if its set of vertices is the set  $P$ .

**Definition 9.3.1** Let  $P = \{p_1, \dots, p_n\}$  be a set of  $n$  points in  $\mathbb{E}^m$ , and let  $\mathcal{V}(P)$  be the Voronoi diagram of  $P$ . We define a complex  $\mathcal{D}(P)$  as follows:

The complex  $\mathcal{D}(P)$  contains the  $k$ -simplex  $\{p_1, \dots, p_{k+1}\}$  iff  $V_1 \cap \dots \cap V_{k+1} \neq \emptyset$ , where  $0 \leq k \leq m$ .

The complex  $\mathcal{D}(P)$  is called the *Delaunay triangulation of the convex hull of  $P$* .

Thus,  $\{p_i, p_j\}$  is an edge iff  $V_i \cap V_j \neq \emptyset$ ,  $\{p_i, p_j, p_h\}$  is a triangle iff  $V_i \cap V_j \cap V_h \neq \emptyset$ ,  $\{p_i, p_j, p_h, p_k\}$  is a tetrahedron iff  $V_i \cap V_j \cap V_h \cap V_k \neq \emptyset$ , etc.

For simplicity, we often write  $\mathcal{D}$  instead of  $\mathcal{D}(P)$ . A Delaunay triangulation for a set of twelve points is shown in Figure 9.11.

Actually, it is not obvious that  $\mathcal{D}(P)$  is a triangulation of the convex hull of  $P$ , but this can be shown, as well as the properties listed in the following lemma.

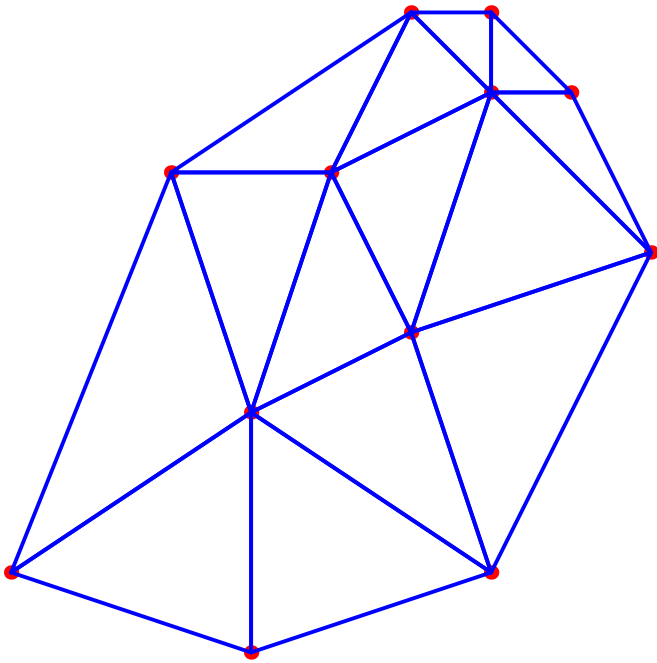


Figure 9.11: A Delaunay triangulation

**Lemma 9.3.2** *Let  $P = \{p_1, \dots, p_n\}$  be a set of  $n$  points in  $\mathbb{E}^m$ , and assume that they are in general position. Then the Delaunay triangulation of the convex hull of  $P$  is indeed a triangulation associated with  $P$ , and it satisfies the following properties:*

- (1) *The boundary of  $\mathcal{D}(P)$  is the convex hull of  $P$ .*
- (2) *A triangulation  $T$  associated with  $P$  is the Delaunay triangulation  $\mathcal{D}(P)$  iff every  $(m - 1)$ -sphere  $S(\sigma)$  circumscribed about an  $m$ -simplex  $\sigma$  of  $T$  contains no other point from  $P$  (i.e., the open ball associated with  $S(\sigma)$  contains no point from  $P$ ).*

The proof can be found in Risler [?] and O'Rourke [?].

In the case of a planar set  $P$ , it can also be shown that the Delaunay triangulation has the property that it maximizes the minimum angle of the triangles involved in any triangulation of  $P$ . However, this does not characterize the Delaunay triangulation.

Given a connected graph in the plane, it can also be shown that any minimal spanning tree is contained in the Delaunay triangulation of the convex hull of the set of vertices of the graph (O'Rourke [?]).

We will now explore briefly the connection between Delaunay triangulations and convex hulls.

## 9.4 Delaunay Triangulations and Convex Hulls

We will see that given a set  $P$  of points in the Euclidean space  $\mathbb{E}^m$  of dimension  $m$ , we can “lift” these points onto a paraboloid living in the space  $\mathbb{E}^{m+1}$  of dimension  $m+1$ , and that the Delaunay triangulation of  $P$  is the projection of the downward-facing faces of the convex hull of the set of lifted points.

This remarkable connection was first discovered by Brown [?], and refined by Edelsbrunner and Seidel [?].

For simplicity, we consider the case of a set  $P$  of points in the plane  $\mathbb{E}^2$ , and we assume that they are in general position.

Consider the paraboloid of revolution of equation  $z = x^2 + y^2$ .

A point  $p = (x, y)$  in the plane is lifted to the point  $l(p) = (X, Y, Z)$  in  $\mathbb{E}^3$ , where  $X = x$ ,  $Y = y$ , and  $Z = x^2 + y^2$ .

The first crucial observation is that a circle in the plane is lifted into a plane curve (an ellipse).

The intersection of the cylinder of revolution consisting of the lines parallel to the  $z$ -axis and passing through a point of the circle  $C$  with the paraboloid  $z = x^2 + y^2$  is a planar curve (an ellipse).

We can compute the convex hull of the set of lifted points. Let us focus on the downward-facing faces of this convex hull.

Let  $(l(p_1), l(p_2), l(p_3))$  be such a face. The points  $p_1, p_2, p_3$  belong to the set  $P$ .

The circle  $C$  circumscribed about  $p_1, p_2, p_3$  lifts to an ellipse passing through  $(l(p_1), l(p_2), l(p_3))$ .

We claim that no other point from  $P$  is inside the circle  $C$ .

Therefore, we have shown that *the projection of the part of the convex hull of the lifted set  $l(P)$  consisting of the downward-facing faces is the Delaunay triangulation of  $P$ .*

Figure 9.12 shows the lifting of the Delaunay triangulation shown earlier.

Another example of the lifting of a Delaunay triangulation is shown in Figure 9.13.

The fact that a Delaunay triangulation can be obtained by projecting a lower convex hull can be used to find efficient algorithms for computing a Delaunay triangulation. It also holds for higher dimensions.

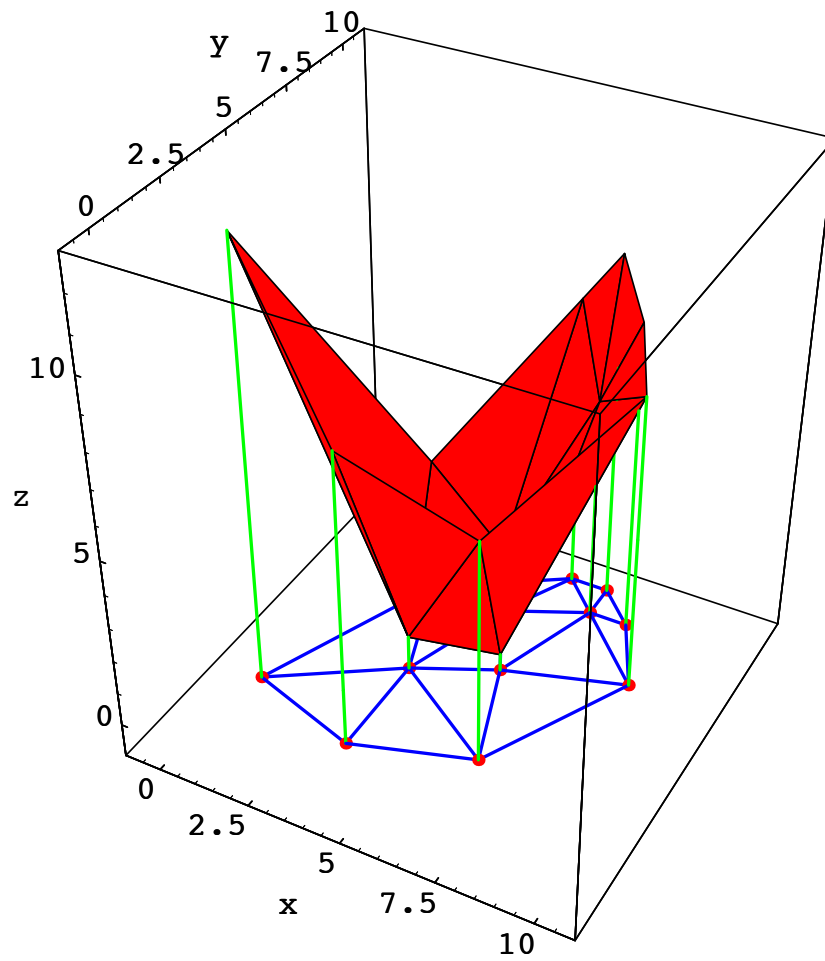


Figure 9.12: A Delaunay triangulation and its lifting to a paraboloid

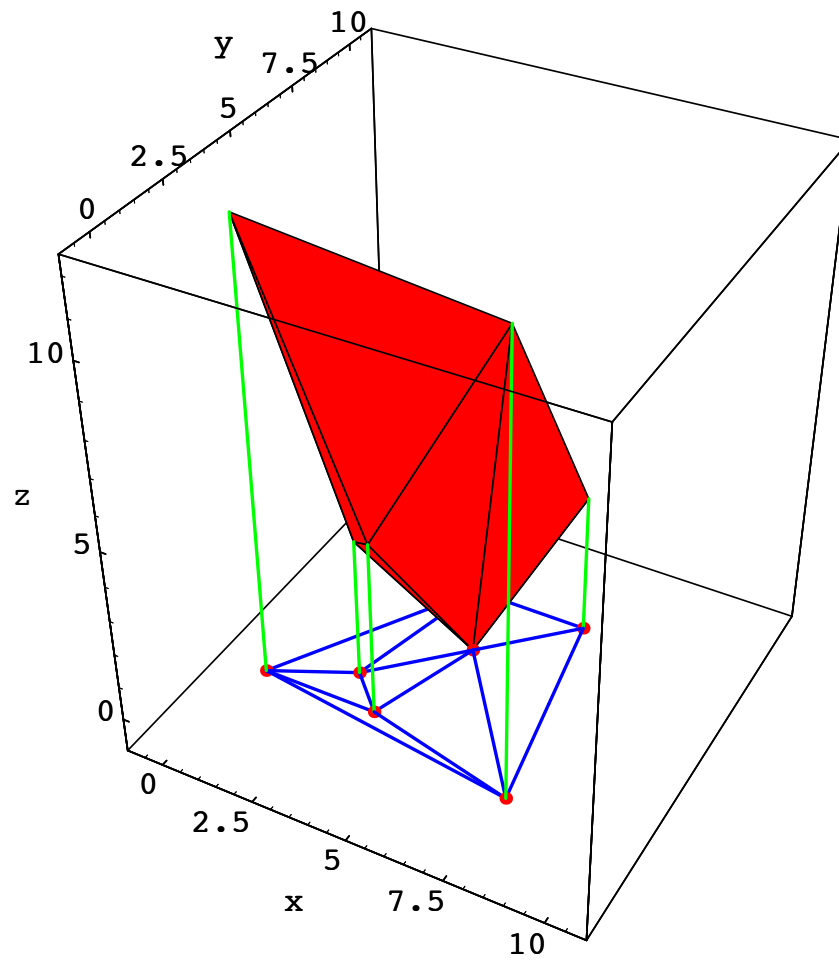


Figure 9.13: Another Delaunay triangulation and its lifting to a paraboloid

The Voronoi diagram itself can also be obtained from the lifted set  $l(P)$ .

However, this time, we need to consider tangent planes to the paraboloid at the lifted points.

It is fairly obvious that the tangent plane at the lifted point  $(a, b, a^2 + b^2)$  is

$$z = 2ax + 2by - (a^2 + b^2).$$

Given two distinct lifted points  $(a_1, b_1, a_1^2 + b_1^2)$  and  $(a_2, b_2, a_2^2 + b_2^2)$ , the intersection of the tangent planes at these points is a line belonging to the plane of equation

$$(b_1 - a_1)x + (b_2 - a_2)y = (b_1^2 + b_2^2)/2 - (a_1^2 + a_2^2)/2.$$

Now, if we project this plane onto the  $xy$ -plane, we see that this is precisely the equation of the bisector line of the two points  $(a_1, b_1)$  and  $(a_2, b_2)$ .

Therefore, *if we look at the paraboloid from  $z = +\infty$  (with the paraboloid transparent), the projection of the tangent planes at the lifted points is the Voronoi diagram!*

It should be noted that the “duality” between the Delaunay triangulation, which is the projection of the convex hull of the lifted set  $l(P)$  viewed from  $z = -\infty$ , and the Voronoi diagram, which is the projection of the tangent planes at the lifted set  $l(P)$  viewed from  $z = +\infty$ , is reminiscent of the polar duality with respect to a quadric.

The reader interested in algorithms for finding Voronoi diagrams and Delaunay triangulations is referred to O’Rourke [?], Preparata and Shamos [?], Boissonnat and Yvinec [?], de Berg, Van Kreveld, Overmars, and Schwarzkopf [?], and Risler [?].

We conclude our brief presentation of Voronoi diagrams and Delaunay triangulations with a short section on applications.

## 9.5 Applications of Voronoi Diagrams and Delaunay Triangulations

The examples below are taken from O'Rourke [?]. Other examples can be found in Preparata and Shamos [?], Boissonnat and Yvinec [?], and de Berg, Van Kreveld, Overmars, and Schwarzkopf [?].

The first example is the *nearest neighbors* problem. There are actually two subproblems: *Nearest neighbor queries* and *all nearest neighbors*.

The nearest neighbor queries problem is as follows: Given a set  $P$  of points and a query point  $q$ , find the nearest neighbor(s) of  $q$  in  $P$ .

This problem can be solved by computing the Voronoi diagram of  $P$  and determining in which Voronoi region  $q$  falls.

This last problem, called *point location*, has been heavily studied (see O'Rourke [?]).

The all neighbors problem is as follows: Given a set  $P$  of points, find the nearest neighbor(s) to all points in  $P$ .

This problem can be solved by building a graph, the *nearest neighbor graph*, for short *nng*. The nodes of this undirected graph are the points in  $P$ , and there is an arc from  $p$  to  $q$  iff  $p$  is a nearest neighbor of  $q$  or vice versa. Then it can be shown that this graph is contained in the Delaunay triangulation of  $P$ .

The second example is the *largest empty circle*.

Some practical applications of this problem are to locate a new store (to avoid competition), or to locate a nuclear plant as far as possible from a set of towns.

More precisely, the problem is as follows. Given a set  $P$  of points, find a largest empty circle whose center is in the (closed) convex hull of  $P$ , empty in that it contains no points from  $P$  inside it, and largest in the sense that there is no other circle with strictly larger radius.

The Voronoi diagram of  $P$  can be used to solve this problem. It can be shown that if the center  $p$  of a largest empty circle is strictly inside the convex hull of  $P$ , then  $p$  coincides with a Voronoi vertex.

However, not every Voronoi vertex is a good candidate. It can also be shown that if the center  $p$  of a largest empty circle lies on the boundary of the convex hull of  $P$ , then  $p$  lies on a Voronoi edge.

The third example is the *minimum spanning tree*.

Given a graph  $G$ , a minimum spanning tree of  $G$  is a subgraph of  $G$  that is a tree, contains every vertex of the graph  $G$ , and minimizes the sum of the lengths of the tree edges.

It can be shown that a minimum spanning tree is a subgraph of the Delaunay triangulation of the vertices of the graph. This can be used to improve algorithms for finding minimum spanning trees, for example Kruskal’s algorithm (see O’Rourke [?]).

We conclude by mentioning that Voronoi diagrams have applications to *motion planning*.

For example, consider the problem of moving a disk on a plane while avoiding a set of polygonal obstacles. If we “extend” the obstacles by the diameter of the disk, the problem reduces to finding a collision-free path between two points in the extended obstacle space.

One needs to generalize the notion of a Voronoi diagram. Indeed, we need to define the distance to an object, and medial curves (consisting of points equidistant to two objects) may no longer be straight lines.

A collision-free path with maximal clearance from the obstacles can be found by moving along the edges of the generalized Voronoi diagram.

This is an active area of research in robotics. For more on this topic, see O'Rourke [?].

